American Journal of Energy and Power Engineering
2018; 5(1): 9-14
http://www.aascit.org/journal/ajepe
ISSN: 2375-3897

American Association for Science and Technology

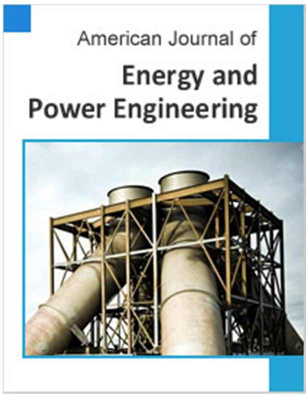

Keywords
Bearing Carrier Frequency,
Amplitude Demodulation,
Envelope Analysis,
Wind Turbine,
Condition Monitoring,
Fault Diagnosis

Received: September 14, 2017
Accepted: November 23, 2017
Published: January 11, 2018

On Bearing Carrier Frequency: Operational Modal Analysis on Wind Turbine Bearing

Ehsan Mollasalehi

Department of Mechanical and Manufacturing Engineering, University of Calgary, Calgary, Alberta, Canada

Email address
emollasa@ucalgary.ca

Citation
Ehsan Mollasalehi. On Bearing Carrier Frequency: Operational Modal Analysis on Wind Turbine Bearing. *American Journal of Energy and Power Engineering.* Vol. 5, No. 1, 2018, pp. 9-14.

Abstract
The objective of this paper is to contribute to the understanding of the bearing carrier frequency. It is widely believed that the carrier frequency of modulating fault frequencies is typically one of the bearing's natural frequencies. To verify this assumption, Operational modal analysis was performed on the bearing vibration signals. Operational modal analysis main assumption is that the excitation of the structure is white Gaussian, which is violated in operating machines. Therefore, the harmonics (shaft and fault harmonics) were removed from the vibration data by converting the time domain signal into the order domain. Results show that the carrier frequency is not necessarily one of bearing's natural frequencies. Out of two main frequency bands excited due to the fault, one included a structural frequency, however the other frequency band did not.

1. Introduction

Bearing fault frequencies appear as sidebands in frequency spectra around a carrier frequency [1]. It is believed that the carrier frequency is typically the resonance frequency of the bearing structure or an element of the bearing [2]. In other words, whenever the rolling elements hit a fault, a sudden impulse is generated, and this impulse excites the resonance frequency of the bearing housing. The excited frequency band in bearings is typically in the kHz range [3]. As shown later in this paper, for generator bearings of a 1.5 MW wind turbine, it is in the range of 2000 to 4000 and 5000 to 7000 Hz. To investigate whether resonance frequencies are excited in these two frequency bands, Operational Modal Analysis (OMA) is used to calculate the natural frequencies of the bearing housing and supporting structure.

However, unlike Experimental Modal Analysis (EMA), the main assumption of OMA is that the excitation of the structure is white Gaussian noise [4], which is basically violated for operating machines specially for a bearing with a fault; because, in addition to the random loads, harmonic excitations are also present due to rotating components. Since the input excitation is not measured in OMA, harmonic excitation (deterministic signals) shall be removed [5], to eliminate the influence of harmonic components in the modal parameter extraction process. It should be noted that harmonic excitation cannot be simply removed by filtering, since it may remove a natural frequency and disguise poles of the system [6].

OMA has been used in variety of applications such as buildings, towers, bridges, etc. where exciting the structure artificially is not possible (see e.g. [7] [8]), and they are excited by wind, traffic, etc. However, there are a few works on operating machines.

The main studies were published by Jacobsen et. al. [9] [10] where he proposed a method using spectral Kurtosis to remove the excitation and transform the measured signal in such a way that it is collected from a broadband excitation. Gade et. al. [6] used the same method for wind turbine gearbox application, where he successfully calculated the modal parameters. There is no other major work to the knowledge of the author.

In this paper, OMA and Frequency Domain Decomposition (FDD) are explained. Then order domain harmonic identification and removal is used to remove the excitation from the signal from a wind turbine generator bearing, to make it suitable for OMA. And finally modal frequencies are calculated to observe whether bearing carrier frequency is one of natural frequencies.

2. Operational Modal Analysis

Modal analysis is a method to determine modal parameters of a system. The system could be a simple structure or a very complex model including several subsystems. Generally, the dynamic behavior of a system such as a vehicle or a wind turbine can be determined from knowledge of its modal characteristics. The response of a linear system to an excitation can be represented as a sum of the contributions from all the modes of the system. The motion and response equation for any linear system is given by:

$$M\ddot{u}(t) + C\,\dot{u}(t) + K\,u(t) = \mathrm{f}(t) \tag{1}$$

where f(t) is the external force on the system. M, C, and K are Mass, damping, and stiffness matrices respectively; u(t) denotes the corresponding acceleration. Each solution of the above equation relates to a Degree Of Freedom (DOF) of the system and the behavior of a small portion of the whole system. When they are combined, they mimic the behavior of the complete system. Classical modal analyses are based on the measurements of both input force and output response, however in many instances input cannot be measured directly, as a result f(t) is not available, and OMA is used in lieu of EMA. Full details of advantage and disadvantage of OMA over EMA can be found in the literature such as [11].

The FDD technique is a non-parametric operational modal analysis technique introduced by Brincker et al. [12]. FDD is based on the singular value decomposition (SVD) on the basis that the excitation is both periodically and spatially white. SVD factorization is represented by:

$$A = U \sum V^{*} \tag{2}$$

where U and V are unitary. $V*$ is the conjugate transpose of V. $\sum$ is a diagonal matrix with real numbers, called singular values on the diagonal.

The relationship between the unknown input (x) and the measured response (y) at the frequency of ω can be written as:

$$G_{yy}(j\omega) = \bar{H}(j\omega) G_{xx}(j\omega) H(j\omega)^{T} \tag{3}$$

where $G_{xx}(j\omega)$ is the r x r power spectral density (PSD) matrix of the input, and r is the number of inputs. $G_{yy}(j\omega)$ is the m x m PSD matrix of the responses, and m is the number of responses. $H(j\omega)$ therefore is the m x r Frequency Response Function (FRF) matrix. An overbar denotes complex conjugate and T represents transpose of the matrix. Since there is no input, and only output data are available, then $m = r$ [13].

On the other hand, the FRF, $H(j\omega)$, can be written in partial fraction form as:

$$H(j\omega) = \sum_{k=1}^{n} \frac{R_k}{j\omega - \lambda_k} + \frac{\bar{R}_k}{j\omega - \bar{\lambda}_k} \tag{4}$$

where n is the number of modes, λ_k is the k^{th}eigenvalue, and R_k is the residue which can be defined as:

$$R_k = \phi_k\, \gamma_k^T \tag{5}$$

where γ_k is the mode shape vector, and ϕ_k is the modal participation vector. γ_k is the transpose of γ [13].

Suppose that the input is a white Gaussian noise, then its PSD is a constant. Substituting $G_{xx}(j\omega) = C$ in eq. (3) gives:

$$G_{yy}(j\omega) = \sum_{k=1}^{n} \sum_{s=1}^{n} \left[\frac{R_k}{j\omega - \lambda_k} + \frac{\bar{R}_k}{j\omega + \bar{\lambda}_k}\right] C \left[\frac{R_s}{j\omega - \lambda_s} + \frac{\bar{R}_s}{j\omega + \bar{\lambda}_s}\right]^H \tag{6}$$

where H indicates the complex conjugate and transpose, i.e. Hermitian [14]. Assuming white Gaussian noise also means that the overall scaling of the system is lost.

Multiplying the two partial fraction matrices and using the Heaviside partial fraction theorem, and after some mathematical manipulations, the output PSD may be shortened to a pole/residue form as:

$$G_{yy}(j\omega) = \sum_{k=1}^{n} \frac{A_k}{j\omega - \lambda_k} + \frac{\bar{A}_k}{j\omega - \bar{\lambda}_k} + \frac{B_k}{-j\omega - \lambda_k} + \frac{\bar{B}_k}{-j\omega - \bar{\lambda}_k} \tag{7}$$

Where A_k is the k^{th} residue matrix of the output PSD [12]. The residue matrix of the output PSD is a m x m Hermitian matrix, given by:

$$A_k = R_k\, C\, \left[\sum_{s=1}^{n} [\frac{\bar{R}_s^T}{-\lambda_k - \bar{\lambda}_s} + \frac{R_s^T}{-\lambda_k - \lambda_s}\right] \tag{8}$$

The contribution to the residue from the k^{th} mode is given by:

$$A_k = \frac{R_k\, C\, \bar{R}_k^T}{2\,\alpha_k} \tag{9}$$

Where α_k is minus the real part of the pole which is $\lambda_k = -\alpha_k + j\omega k$. When the damping is light, the residue becomes proportional to the mode shape vector:

$$A_k \simeq R_k\, C\, \bar{R}_k = \phi_k \gamma_k^T\, C\, \gamma_k \phi_k^T = d_k \phi_k \phi_k^T \tag{10}$$

where d_k is a scalar constant [11]. At a certain frequency ω, only a limited number of modes will dominate significantly, typically one or two. Let this set of modes be denoted by Sub(ω). Therefore, in the case of a lightly damped structure, the response spectral density can be written as:

$$G_{yy}(j\omega) = \sum_{k \in Sub(\omega)} \frac{d_k \phi_k \phi_k^T}{j\omega - \lambda_k} + \frac{\bar{d}_k \bar{\phi}_k \bar{\phi}_k^T}{j\omega - \bar{\lambda}_k} \tag{11}$$

[13]. This final form of the matrix is then decomposed into a set of singular values and singular vectors using SVD.

To implement the practical FDD technique, the first step is to estimate the PSD matrix. The calculation of the output PSD ($G_{yy}(j\omega)$) at discrete frequencies ($\omega = \omega_i$) is then decomposed by taking SVD of the matrix:

$$G_{yy}(j\omega) = U_i S_i V_i^T \tag{12}$$

[12]. It should be noted that, in the case of real valued matrices, the V^* is a simple transpose. Near the peak corresponding to the k^{th} mode in the spectrum, the eigenvalue will dominate in its neighborhood. If only the k^{th} mode is dominating there will only be one term in eq. (11). Thus, in this case, the first singular vector u_{i1} is an estimate of the mode shape:

$$\phi = u_{i1} \tag{13}$$

and the corresponding singular value is the auto-power spectral density function of the corresponding single degree of freedom system. The PSD ($G_{yy}(j\omega)$) function is identified close the peak by comparing the mode shape estimate ϕ with the singular vectors for the frequency lines around the peak.

3. Harmonic Identification and Removal

There are two main approaches to identify the deterministic harmonics. First being Kurtosis as explained in [9], called Extended Kurtosis Checking. The idea is that the power spectral density function for a structural mode excited by a broadband signal is different from the one excited by a deterministic signal. Therefore, for each frequency line, the Kurtosis is calculated and compared with mean Kurtosis of other measurements at the same frequency line. Theoretically, if the signal is purely Gaussian distributed the mean is 3. If the Kurtosis deviates significantly from the mean Kurtosis, then the distribution is different from other measurements, and therefore should not be included in the OMA analysis.

The second approach is explained in [15]. The overall concept is to change the time domain to angular domain, remove the known harmonic orders, and reconstruct the signal in time domain. This method is suitable for bearing vibration signal in wind turbines, since bearing characteristic orders are known based on the geometry. To examine the approach, a bearing signal is simulated. The simulated bearing has five rolling elements, with diameter of 2 cm and pitch diameter of 10.5 cm; thus, the outer race impulse frequency is $2f_s$ Hz, that is the second order of shaft rotational speed. The impulse excitation can be considered as a defect input to the system that excites the natural frequency of the system when balls pass the defect. The bearing assembly is assumed to be a second order system as:

$$h(\boldsymbol{s}) = \frac{K\,\omega_n^2}{s^2 + 2\xi\omega_n s + \omega_n^2} \tag{14}$$

This second-order impulse response is expressed in Laplace domain where K, ξ, and ω are DC-gain of the function, damping coefficient and natural frequency of the system, respectively. Any second order system whose transfer function is in the form of eq. (14) is stable for any positive values of ξ and ω. The time response of the second order system to an impulse input can be solved explicitly. The response in the frequency domain can be obtained as the product of the system transfer function and the Laplace transform of the unit step input signal, which is one (1) in case of impulse excitation to the system. The overall signal simulated from a bearing, then, can be created by adding the shaft harmonic and structural response (considering no noise). The natural frequencies of the system are assumed to be 104 and 217 Hz. The fault is on the outer race (fixed position), and therefore, every time a rolling element hits it, an impulse is generated. The rotational speed is considered to be 5 Hz. Figure 1 shows the spectrum of the simulated signal.

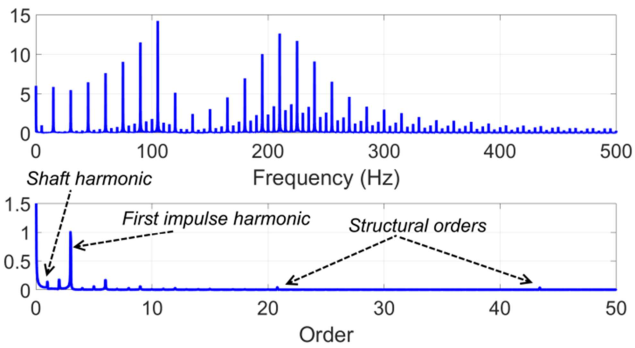

Figure 1. *(Top) FFT spectrum of the simulated signal, (Bottom) Order spectrum of the same signal.*

Speed frequency and its harmonics are noticeable, as well as fault impulse frequency which is twice the speed frequency. The spectrum magnitude increases around the defined natural frequencies. To summarize, there are three components in the signal, shaft harmonics, modulating impulse components, and structural frequency components. The first two are violating the OMA assumption (i.e. white Gaussian excitation) and shall be removed, and only the fixed structural frequency components to be kept. To remove harmonic components caused by shaft speed and impulses, the signal is converted to angular domain, and FFT is applied on the constant angle sampled data ($x(\theta_r)$) as shown in the same figure, using:

$$X(O_n) = \sum_{r=0}^{N-1} x(\theta_r) e^{-i(2\pi nr/N)} \tag{15}$$

Shaft speed harmonics are clearly noticeable. Impulse orders have higher magnitude. Orders excited at natural frequencies have much lower magnitudes. An index is defined as:

$$k = j(\Delta\theta\ O) \tag{16}$$

where j is an integer and O is order number. Thus, harmonics at k_s in the order spectrum need to be removed. It is important to keep both the real and imaginary values of the spectrum, when an order is removed, because an inverse Fourier transform will be applied later to reconstruct the signal. If direct zeroing was applied, the signal characteristics would also be removed.

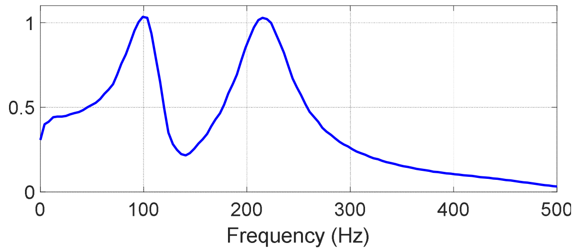

Figure 2. *Spectrum of the reconstructed simulated signal after harmonics were removed.*

Moreover, if the fixed structural frequency component happens to be on the variable harmonic, it will be removed, which is against the purpose of OMA. As a result, the local average values are used around the order which is to be removed:

$$X(O_k) = \frac{Re[X(O_{k-1})]+Re[X(O_{k+1})]}{2} + \frac{Im[X(O_{k-1})]+Im[X(O_{k+1})]}{2} \quad (17)$$

It should be noted that *j* in eq. (16) starts from the upper limit of $N/\Delta\theta O$ and decreases to 1. After the harmonics of the shaft and impulses are removed, the remaining components are used to reconstruct the signal in time domain using fixed time steps. The result is shown in figure 2. It clearly shows the defined natural frequencies, and harmonics were effectively removed.

4. Bearing Vibration Analysis

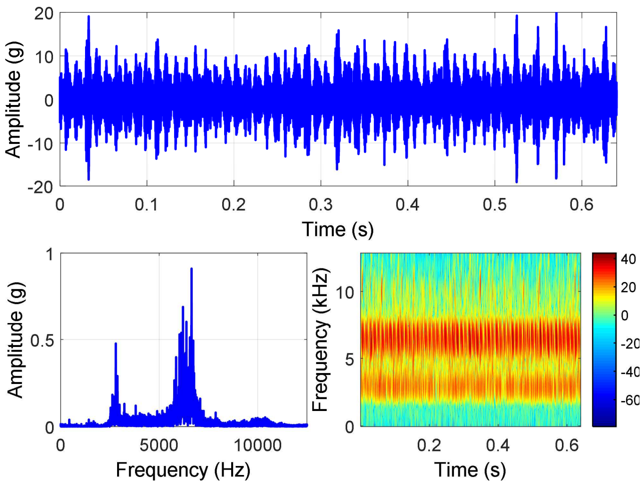

Figure 3. *(Top) Raw acceleration data, (Bottom left) FFT Spectrum, (Bottom right) Spectrogram, at 1435 RPM- color scale (z-axis) represents the spectrogram amplitude (g).*

The wind turbine generator bearing studied in this paper had high value of vibration RMS, around 4 g. Figure 3 represents the raw acceleration data, sampled at 25.6 kHz, when the shaft rotational speed was 1435 RPM, FFT spectrum and also the Short-time Fourier Transform (STFT) plot of one data (that is typical of other sets of data for this turbine). It is apparent that there are two main clusters, one around 6000 Hz which is the bearing natural frequency range, and the other one is around 3000 Hz. Therefore, the amplitude demodulation technique was performed on both frequency bands, as shown in figure 4. The sideband frequency and the harmonics in both top and bottom figures are associated with the ball pass frequency of outer race (BPFO), therefore, it is most likely that the bearing has a defect on its outer race.

5. Operational Modal Analysis on Bearing Vibration Data

As mentioned, vibration signals from the bearing contain three main parts; shaft harmonics, fault frequency harmonics, and structural vibration. There is a fourth part which is noise and frequency components from other rotating components close to the bearing vibration sensor in wind turbine drive-train. Structural frequencies are fixed theoretically, since they are directly related to the structure and not affected by the shaft rotational speed. On the other hand, fault frequencies (bearing characteristic frequencies) are directly related to the shaft speed, and can be represented as multiples of the first order (which is shaft order). Therefore, to remove these harmonics, the following steps are applied to the signal:

a. Vibration signal is converted to angular domain using computed order resampling
b. The resampled signal is transformed to order domain
c. Shaft orders and bearing characteristic orders are removed using the *k* index
d. The remaining orders are transformed back to the time domain
e. The reconstructed time domain signal is used for OMA

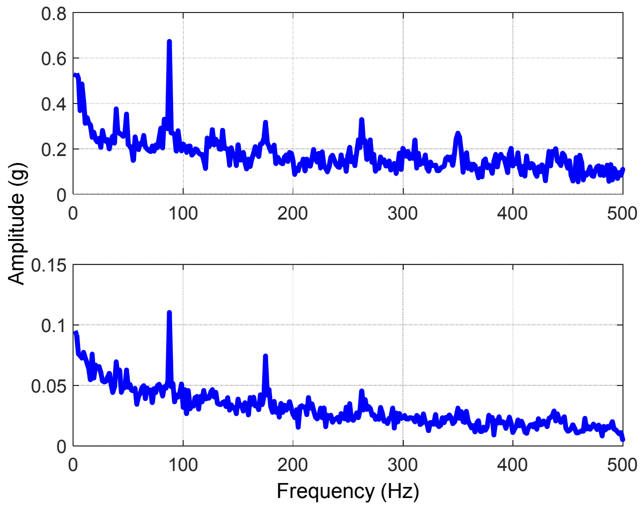

Figure 4. *Amplitude demodulation of (Top) 2000-4000 Hz, (Bottom) 5000-7000 Hz.*

Four accelerometers are attached on the bearing housings, two on drive end bearing, and two on non-drive end bearing. Vibration data are transformed into the angular domain (order tracking) and outer race and shaft orders are removed. Based on the geometry of the bearing (n=9, d=4.5 cm, D=23.5 cm, and α=0◦), the outer race frequency order is:

$$O_{BPFO} = \frac{n}{2}\left(1 - \frac{d}{D}\cos\alpha\right) = 3.64 \quad (18)$$

It should be noted that the bearing does not purely roll. The slide-roll ratio is typically 2-3% [16], thus eq. (18) only suggests the neighborhood of the outer race fault order. In order to remove the exact fault harmonic effectively, each vibration signal is analyzed separately. Figure 5 shows a sample of the order diagram. The first order and integer harmonics relate to the shaft speed, whereas the order of 3.6 and its first three multiples relate to the outer race fault. Once the rotating orders are removed, the signals are converted back to time domain for further OMA analysis. Figure 6 shows the signal spectrum (a moving average filter is used to eliminate high frequency Gaussian components) after orders are effectively removed.

To start extracting the modal parameters by OMA, FDD is used. There are no measured input signals, and Cross Spectral Densities (CSD) between outputs, f and g at sequence n is:

$$CSD_{fg}(n) = \sum_{m=-\infty}^{\infty} \bar{f}[m]g[n+m] \quad (19)$$

where $\bar{f}$ denotes the complex conjugate of f in the frequency domain [17]. For N channels, a matrix is created as:

$$G_{yy}(j\omega) = \begin{bmatrix} PSD_{1,1} & \cdots & CSD_{1,N} \\ \vdots & \ddots & \vdots \\ CSD_{N,1} & \cdots & PSD_{N,N} \end{bmatrix} \quad (20)$$

where diagonal elements, PSD, represent cross-correlation between same measurements called auto-correlation, and CSD, off-diagonal elements, represent cross-correlation between different measurements [8]. And finally, SVD is applied for each frequency, and repeated for the number of the measurements. This algorithm was validated by the author in [18], where an Euler-Bernoulli beam was modeled and time domain data from a free vibration analysis was simulated. An initial detection was made at the end of the beam and the responses at five locations (spaced equally along the beam) were calculated. The simulated time domain vibrations were inserted to the FDD algorithm, and it was shown that the FDD results are in agreement with the results from the simulation.

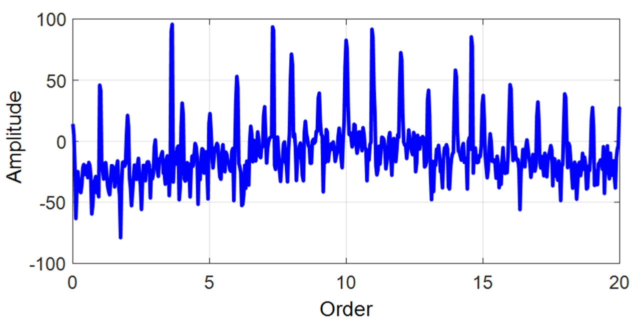

Figure 5. *Sample of order analysis on the generator bearing vibration data.*

Non-drive end generator bearings can potentially act as reference channels since they are minimally corrupted with fault frequencies from the drive end bearing signal. Subsequently, only shaft harmonics are removed from non-drive end bearing. Figure 7 presents normalized (to the maximum value yielding the maximum of 1) singular values calculated by FDD. Since the data acquisition period is short, the low frequency values might not represent all structural frequencies. Regardless, two frequency bands are important in this analysis: 2000 to 4000 Hz and 5000 to 7000 Hz. For the frequency band of 2000 to 4000 Hz, there is a main peak excited close to 4000 Hz, which acted as carrier frequency in the presence of a fault. For the frequency band of 5000 to 7000 Hz, there are no major peaks, this suggests that fault frequencies at this frequency band do not excite any structural frequencies. That said, the OMA assumptions are not completely met in this analysis. For instance, harmonic excitations from other rotating equipment (such as harmonics from the gearbox) might still be present in the signals after shaft and fault order were removed; It is minimum in non-drive end bearing.

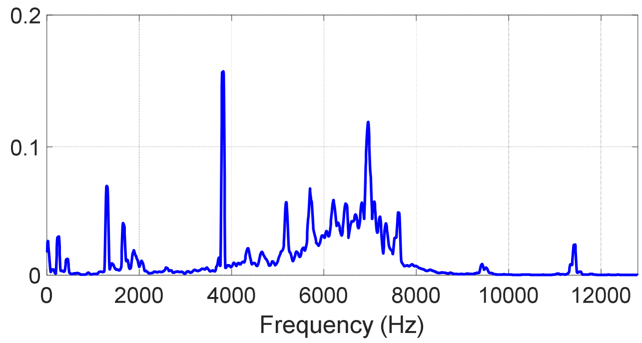

Figure 6. *Bearing signal spectrum after harmonics were removed.*

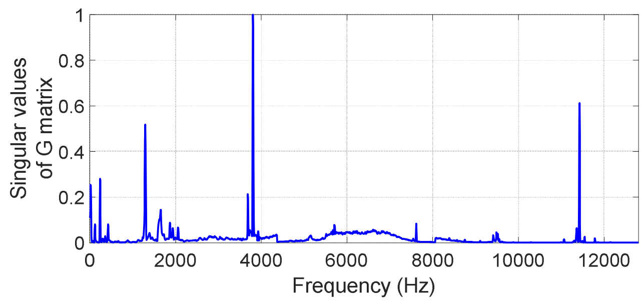

Figure 7. *Normalized excited frequencies for the entire bearing datasets.*

Or, modal analysis is established under the assumption that the structure behavior is linear. Therefore, the results are not completely firm, yet they suggest more works and investigations on the understanding of the carrier frequency definition.

6. Conclusions

It is believed that bearing fault impulses excite a natural frequency of the bearing structure, in other words the carrier frequency of the modulating impulses is one of the natural frequencies. To investigate this, operational modal analysis was used to calculate the structural frequencies of the bearing and its supporting structure. OMA, also called as output-only modal analysis, is based on measuring the output of a system and using the ambient and natural operating forces as unmeasured input. Thus, OMA assumption is that the excitations of the system are white Gaussian signal, and harmonic excitations (which potentially are mistaken for being structural modes) are to be removed before OMA analysis. Order spectrum was used to remove the known harmonic components of the signals: vibration signals were represented in angular domain, and known harmonics (shaft and fault orders) were removed by local averaging. Then, the order spectrum was converted back to frequency domain, and finally time domain signal was reconstructed, and OMA was applied.

The analysis was applied to wind turbine generator bearings. Generator bearing faults excite mainly two frequency bands in kHz range (i.e. 2-4 kHz and 5-7 kHz). The results obtained from the OMA showed that the first frequency band contains a structural frequency, but the second band does not. Although analyses in this paper has a few uncertainties (e.g. other harmonics from other components in the drive-train might still be present in the reconstructed signal), the result suggests that modulating fault impacts to the bearing do not necessarily excite natural frequencies of the structure.

Acknowledgements

This research was supported by the Natural Science and Engineering Research Council of Canada (NSERC) under the Industrial Research Chair program, and the Research and Development Engage program. We thank TransAlta Corp. for providing the bearing vibration data.

References

[1] E. Mollasalehi, Q. Sun, D. Wood, Wind turbine generator bearing fault diagnosis using amplitude and phase demodulation techniques for small speed variations, Advances in Condition Monitoring of Machinery in Non-Stationary Operations (2016) 385-397.

[2] P. McFadden, J. Smith, Vibration monitoring of rolling element bearings by the high-frequency resonance technique-a review, Tribology international 17 (1) (1984) 3-10.

[3] S. Lacey, An overview of bearing vibration analysis, Maintenance & Asset Management 23 (6) (2008) 32-42.

[4] J. Brownjohn, F. Magalhaes, E. Caetano, A. Cunha, Ambient vibration retesting and operational modal analysis of the humber bridge, Engineering Structures 32 (8) (2010) 2003-2018.

[5] B. Peeters, B. Cornelis, K. Janssens, H. Van der Auweraer, Removing disturbing harmonics in operational modal analysis, in: Proceedings of International Operational Modal Analysis Conference, Copenhagen, Denmark, 2007.

[6] S. Gade, R. Schlombs, C. Hundeck, C. Fenselau, Operational modal analysis on a wind turbine gearbox, in: Conference & Exposition on Structural Dynamics, 2009.

[7] B. Peeters, G. De Roeck, Stochastic system identification for operational modal analysis: a review, Journal of Dynamic Systems, Measurement, and Control 123 (4) (2001) 659-667.

[8] E. Mollasalehi, Q. Sun, D. Wood, Contribution of small wind turbine structural vibration to noise emission, Energies 6 (8) (2013) 3669-3691.

[9] N.-J. Jacobsen, P. Andersen, R. Brincker, Applications of frequency domain curve-fitting in the EFDD technique, in: Proceedings IMAC XXVI Conference, 2008.

[10] N.-J. Jacobsen, P. Andersen, R. Brincker, Eliminating the influence of harmonic components in operational modal analysis, in: Proceedings IMAC XXV Conference, 2007.

[11] R. Brincker, L. Zhang, P. Andersen, Modal identification of output-only systems using frequency domain decomposition, Smart materials and structures 10 (3) (2001) 441.

[12] R. Brincker, L. Zhang, P. Andersen, Modal identification from ambient responses using frequency domain decomposition, in: Proc. of the 18 International Modal Analysis Conference (IMAC), San Antonio, Texas, 2000.

[13] M. Batel, Operational modal analysis-another way of doing modal testing, Sound and Vibration 36 (8) (2002) 22-27.

[14] F. Shen, M. Zheng, D. F. Shi, F. Xu, Using the cross-correlation technique to extract modal parameters on response-only data, Journal of sound and vibration 259 (5) (2003) 1163-1179.

[15] C. L. Groover, M. W. Trethewey, K. P. Maynard, M. S. Lebold, Removal of order domain content in rotating equipment signals by double resampling, Mechanical Systems and Signal Processing 19 (3) (2005) 483-500.

[16] R. B. Randall, Vibration-based condition monitoring: industrial, aerospace and automotive applications, John Wiley & Sons, 2011.

[17] R. Bracewell, P. B. Kahn, The Fourier transform and its applications, American Journal of Physics 34 (8) (1966) 712-712.

[18] E. Mollasalehi, Small wind turbine tower vibration and noise emission (2013).